Grazing incidence optics for X-ray astronomy: X-ray optics

Article *in* Journal of Optics · September 2011

DOI: 10.1007/s12596-011-0040-2

K P Singh
Tata Institute of Fundamental Research

J Opt (July-September 2011) 40(3):88–95
DOI 10.1007/s12596-011-0040-2

RESEARCH ARTICLE

Grazing incidence optics for X-ray astronomy

X-ray optics

Kulinder Pal Singh

Received: 18 April 2011 / Accepted: 5 August 2011 / Published online: 26 August 2011

Abstract Cosmic X-ray sources are usually very weak and their detection, therefore, needs large area telescopes to gather light and sensitive detectors to enhance quantum efficiency. Conventional telescopes for visible light use refracting or reflective optics which is impractical for X-ray wavelengths because photon energies are greater than the binding energies of the typical atomic electrons leading to a refractive index for X-rays being less than unity. Thus single surface reflectivity for near-normal incidence is negligible for X-rays. However, by Snell's Laws, total external reflection occurs and X-rays can be reflected from a surface up to a critical angle (usually about a degree for energies below 10 keV) given by cosine $\theta = n$. This is known as the grazing angle. X-ray telescopes are made to exploit the grazing incidence from a set of co-axial and confocal shells of paraboloidal and hyperboloidal mirrors. X-ray reflectors having high atomic number surfaces with low scattering are used to realize imaging capability for a telescope. I describe here various configurations required, and the various technologies used and their limitations, to make practical X-ray telescopes. A soft X-ray imaging telescope (SXT) using grazing incidence has been built at TIFR for ASTROSAT—an Indian Multiwavelength Satellite designed to cover a very broad band of X-rays, UV and optical. Astrosat is planned to be launched by a Polar Satellite Launch Vehicle in 2012 into a near-Earth Equatorial orbit. I will also describe the ongoing R&D for realizing telescopes for hard X-rays above 10 keV useful for both Astronomy and medical diagnostics.

Keywords X-ray optics · X-ray telescopes · X-ray astronomy

Introduction

X-ray telescopes based on grazing incidence provide the necessary high sensitivity for X-ray observations by virtue of their direct imaging capability and reduction of the non-Xray background levels encountered in space. Optics thus built has transformed the field of observational X-ray astronomy into a major scientific discipline at the cutting edge

The paper was based on presentation at XXXV OSI symposium held at Thiruvananthapuram during 16–18 January 2011.

K. P. Singh (✉)
Dept. of Astron. & Astrophys., Tata Institute of Fundamental Research, Homi Bhabha Road, Mumbai 400005, India
e-mail: singh@tifr.res.in

of research in astrophysics and cosmology, in a relatively short time span of just a few decades [1]. Probing the hottest and extreme conditions of gravity and magnetic field, X-ray astronomy has led to many discoveries and detection of new phenomena. X-rays have been detected from essentially every type of astronomical object: accreting binary stars with compact companions like neutron stars, black-holes and white dwarfs, million to a billion degree hot gas in intra-cluster medium in clusters of galaxies, stellar coronae, shock heated remnants of supernovae, and accreting black-holes believed to exist in the centers of quasars.

X-ray reflection

X-rays can interact with the atoms in the matter through absorption, scattering, diffraction, reflection, transmission, refraction and re-radiation via flourescence or emission of Auger electrons. The interaction of X-ray wavelengths can be described by using Maxwell's equations, and the scattering cross-sections for free electrons as well as bound electrons in an atom can be calculated. It is important to remember that X-ray wavelenghts are very short and comparable to the atomic dimensions, and the photon energies comparable to the binding energies of the electrons in atoms. The matter, however, consists of several atoms each with several electrons complicating the problem. In general, the refractive index of a material for incident X-rays is estimated assuming propagation in the forward direction and by calculating the sum of all the forward scattered waves interefering with the incident wave. The refractive index depends on wavelength particularly near the resonances (or shell binding energies) and is thus said to be dispersive. For frequencies (ω) greater than the resonance frequency (ω_s) the refractive index n(ω) is slightly less than 1 leading to anomalous dispersion. The refractive index is commonly written as $n(\omega) = 1 - \delta + \iota\beta$, where the imaginary part describes the absorption, and

$$\delta = (2\pi)^{-1} n_e r_e \lambda^2 f_1^0(\omega) \tag{1}$$

$$\beta = (2\pi)^{-1} n_e r_e \lambda^2 f_2^0(\omega) \tag{2}$$

where f_1 and f_2 are the atomic scattering factors, n_e and r_e are the electron density and the electron radius respectively.

Since for X-rays the refractive index is very close to unity, the reflectivity at most angles of incidence is negligible. However, for the radiation incident at grazing angle to the surface (far from the normal incidence) the reflectivity is nearly complete. This is known as total external reflection and is used for X-ray focussing. This can be seen easily using the Snell's law, according to which the visible light will be bent towards the surface normal when entering a medium of refractive index greater than unity. For X-rays incident at near grazing angle to the surface the angle of refraction can equal $\pi/2$, indicating that the refracted wave does not penetrate the surface, and instead travels along the surface. Assuming that β is negligible it can be shown that there is a critical angle, θ_c from the surface plane for which total external reflection occurs. The critical angle is given by

$$\cos\theta_c = 1 - \delta \tag{3}$$

Since δ is very small for X-rays, the above equations leads to

$$\theta_c = (2\delta)^{1/2} \tag{4}$$

where

$$\delta = \left(N_0 Z r_e \rho \lambda^2\right) / A 2\pi \tag{5}$$

Here, Z is the atomic number of the surface, A is the atomic weight, ρ is its density, λ is the wavelength of the incident X-rays, and N_0 is the Avogadro's number. For heavy elements, Z / A = 0.5, thus

$$\theta_c = 5.6\lambda\rho^{1/2}\text{arcmin} \tag{6}$$

Here, λ is in Angstroms, and ρ is in gm/cm^3. Typical metals used for X-ray reflection are smooth surfaces of nickel, gold, platinum or iridium. Thus θ_c is about a degree for typical X-ray wavelengths and is proportional to $\rho^{1/2}$/E where E is the photon energy of the X-rays. This was first demonstrated by Arthur Compton in 1922.

A more detailed description of this can be found in the book by D. Attwood [2]. The reader is also referred to a general article on X-ray Optics and its uses in various subjects written by Underwood and Attwood [3]

X-ray telescope geometries

It is well known that a concave spherical mirror at near-normal incidence forms a good image of a point object on the optical axis. However, as the object moves away from the axis the image starts to get elongated. At glancing incidence required for X-rays, this astigmatism is extreme: The image of a point becomes a line. Thus, a single spherical mirror is not a useful imaging device for X-rays. Therefore, special geometries are required for making a truly imaging system. An excellent description of the various X-ray telescopes and the geometries used is given in a review article by Aschenbach [4]. A summary is given below.

Kirkpatrick and Baez optics

The first 2-dimensional X-ray images in the laboratory were made in 1948 using 2 sets of parabolic sheet mirrors (parabolas of translation) with axes of revolution perpendicular to each other. Here, light emerging from the front mirror was intercepted by the rear mirror (Fig. 1). The rays shown as red lines are the tangential (meridional) rays for the front mirror and are strongly focused by it, but weakly focused by the rear mirror for which these rays become the sagiital rays. The blue rays are the sagittal rays for the front mirror. Each mirror corrects the astigmatism of the other. A spatial resolution of 5–10 arcsecs for on-axis, and 1 arcmin for X-rays one degree off-axis, was achieved.

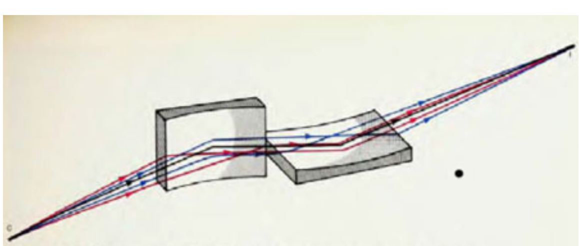

Fig. 1 Kirkpatrick–Baez optics that corrects the astigmatism associated with grazing-incidence spherical mirrors

This kind of optics is known as the Kirkpatrick–Baez optics [5] and is used in X-ray microscopes and used to image the laser-fusion experiments. In order to increase the collecting area for a telescope a stack of parabolas of translation is constructed by placing a number of such mirrors parallel to each other.

Wolter optics

A parabola of revolution (rotating the parabola around its central axis) will focus only the on-axis rays. Off-axis rays (off-axis by angle δ) will focus on a ring of radius Fδ. In two remarkable papers in 1952, H Wolter [6, 7] described a series of designs and geometries for such X-ray telescopes. He showed that no single mirror configuration can give a 2-D focusing over a field and that an even number of surfaces are needed. The one most commonly used consists of a set of co-axial and con-focal shells of paraboloidal and hyperboloidal mirrors where X-rays are first reflected by an internally reflecting paraboloidal mirror and then reflected to the prime focus of the telescope by the internally reflecting hyperboloid mirror (Fig. 2). Focal length is measured from the mid point of the paraboloid and the hyperboloid. This geometry is known as Wolter I optics and is most commonly used in all X-ray telescopes since the optical system has the shortest dimension in this configuration with respect to Wolter Type II or Type III configurations shown in Fig. 3. A grazing incidence telescope acts as a thin lens. As the telescope tilts about small angles, the image of a point

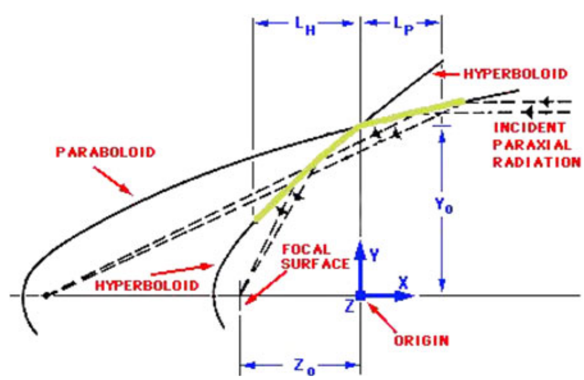

Fig. 2 Wolter Type I optics for grazing-incidence mirrors

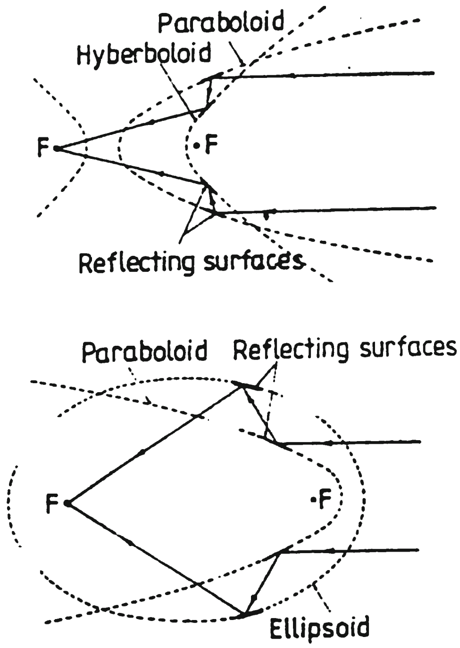

Fig. 3 Wolter Types II and III optics for grazing-incidence mirrors

source near the axis remains invariant in space. This is what allows us to convert a linear distance y between two images to an angular distance θ= y/F. This shows that the optimum focal surface is a bowl shape, sitting on the flat plane perpendicular to the optical axis. In a Wolter I system the rays from an on-axis point source converge to focus in a cone of half-angle four times the grazing angle.

At grazing incidence, the active region of the mirror is just a thin annulus giving a small collecting area even for a large diameter mirror. Therefore, several Wolter I shells are nested like Russian dolls to improve the filling factor of the circle defined by the outermost shell, and thus increase the reflecting areas, as in Fig. 4 which shows the schematic of a practical system used in the XMM-Newton X-ray telescopes.

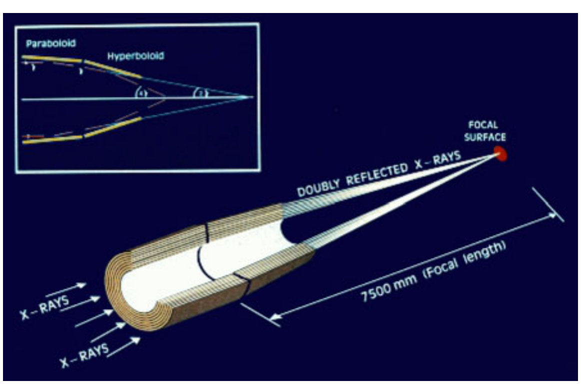

Fig. 4 Nested Wolter Type I optics for XMM-Newton X-ray telescopes

Fabrication technologies for X-ray telescopes

Telescopes for soft X-rays in the energy range of 0.1 to 10 keV have been built based on Wolter I geometry and have provided X-ray images with arcsec to sub-arcsec resolution that have revolutionized X-ray astronomy. The mirrors in each of these observatories namely, Einstein, ROSAT and Chandra, were figured to perfect paraboloid and hyperboloid shapes by diamond turning of thick material like Zerodur (glass with zero thermal expansion) to provide stiffness for maintaining the perfect shape. Figure 5 shows the grinding of one of the mirrors for Chandra X-ray observatory (CXO). These mirrors are then polished and coated with a high Z material (iridium in case of CXO).

A much higher nesting (40 to 120 mirrors) within the same aperture or diameter (usually ranging between 140–700 mm) of the largest paraboloid can be achieved by using substrates made of thin foils [8, 9]. Use of thin foils leads to (a) savings in

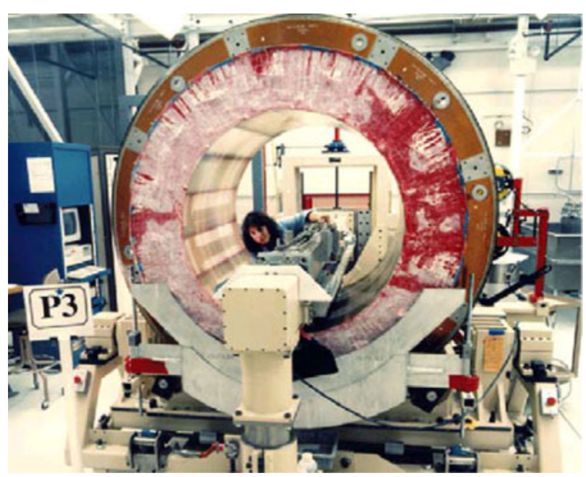

Fig. 5 Grinding of Chandra mirrors

weight that is very important for a satellite mission, (b) savings in cost due to the ease of fabrication, as expensive diamond turning and figuring are not required, and (c) higher upper energy limit, since thin foils can be nested closer to the axis giving smaller grazing angles for reflecting higher energy photons. For example, the X-ray mirrors in XMM-Newton are gold-coated nickel shells and are produced via replication process as shown in Fig. 6. A gold layer deposited on a highly polished master mandrel is transferred to the nickel shell that is electroformed on the gold layer. The master mandrels are made from double conical Al blocks coated with Ni and lapped to exact paraboloid and hyperboloid shapes of Wolter I geometry, and then superpolished to reduce scattering.

The X-ray telescopes in ASCA (1993, Japan and USA), Suzaku (Japan and USA) and the SXT on ASTROSAT (India) have even thinner (0.15–0.2 mm) foils of gold-coated Al but shaped in a conical approximation to Wolter I optics. The number of concentric mirror shells is 120 in ASCA, 168 in ASTRO-E2, and 40 in SXT. This results in even higher savings in weight (only 10–20 kg for a mirror module compared to 484 Kg for XMM and 1480 Kg for Chandra) but the spatial resolution obtainable with such telescopes is a few arcmin. In ASCA gold was deposited by evaporation and the surface was given a lacquer coating. Several improvements were made in Suzaku by using replication process [10–13] where a layer of gold deposited by sputtering on a smooth glass is transferred to Al via an epoxy coupling layer, thus replicating the smoothness of the glass surface on to the gold layer. The entire process is described

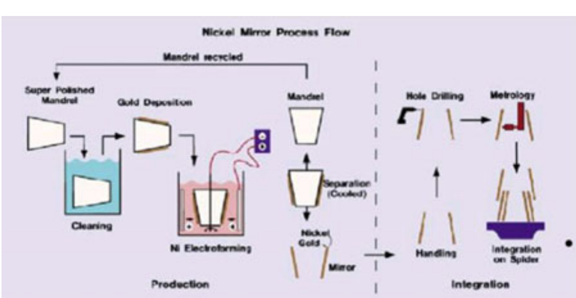

Fig. 6 Replication technology used for making complete mirror shells for XMM-Newton

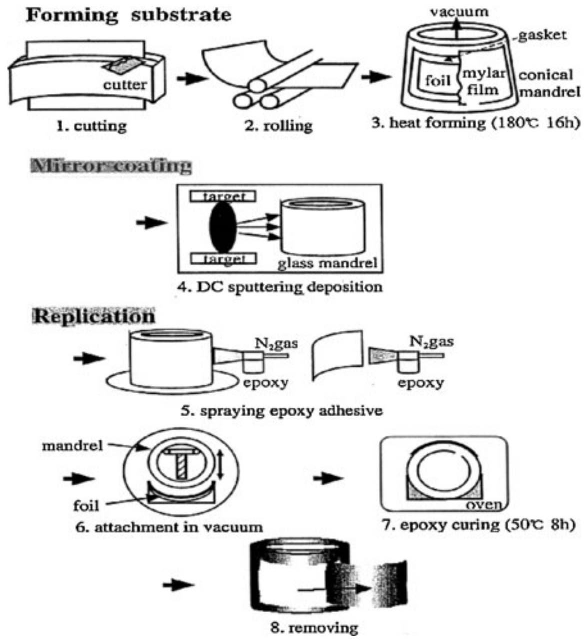

Fig. 7 Replication technology used for making quadrants of mirror shells for Suzaku and Astrosat

in Fig. 7, and was also used for making mirrors for SXT at TIFR.

X-ray surface scattering measurements

The uniformity and smoothness of the reflective coating is critical to imaging performance of the optics, since irregularities in the mirror surfaces can cause light to be scattered out of the core of the X-ray image, degrading the angular resolution of the telescope. Highly smooth surfaces are thus a pre-requisite for good imaging in an X-ray telescope. Most importantly, the reflection efficiency of an X-ray telescope is strongly dependent on energy due to the presence of atomic absorption edges and the rapid decrease in efficiency at high energies. Scattering is predominantly in the plane of the incident X-rays and normal to the surface. Out of plane scattering is less by a factor of sineα where α is the incident angle. Scattering is asymmteric. Backward scattering is no more than $-\alpha$ whereas forward scattering is unlimited. For details of scattering theories the reader is referred to [4, 14] and references therein. The scattering is measured by studying the reflectivity

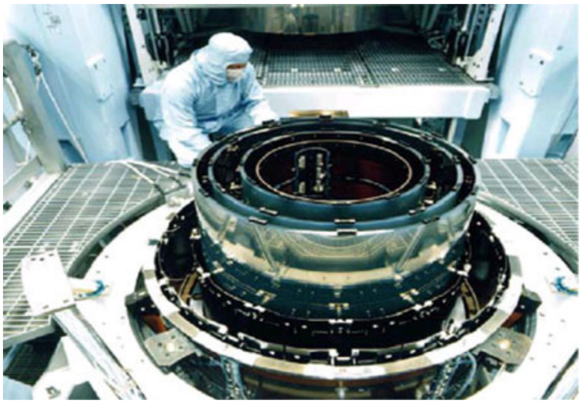

Fig. 8 Assembly of four nested shells of Chandra mirrors

of the X-ray mirrors as a function of incident angles within the grazing angles and modeling the reflectivity curves thus obtained. The modeling leads to the surface roughness parameter which indicates the quality of the surface and its scattering properties. One such set of measurements were carried out by us for X-ray mirrors developed in TIFR and are described in [15]. The surface roughness expressed in terms of scale heights of irregularities was determined to be 10 Angstroms for SXT, comparable to the mirrors for Suzaku. The XMM-Newton mirrors have roughness of 4 Angstroms, whereas the Chandra mirrors are the smoothest mirrors ever made so far.

Examples of X-ray telescopes and X-ray images of the universe

Figures 8, 9, 10 and 11 show three examples of X-ray telescopes, viz., Chandra X-ray Observatory with four nested mirrors and 10 m focal length, XMM-Newton telescope with 58 nested mirrors and 8 m focal length, and a Soft X-ray Telescope (SXT) with 40 nested shells and 2 m focal length for India's first Astronomy satellite, ASTROSAT to be launched in 2012. The combination of the smoothness of the mirrors, their adherence to the exact paraboloid and hyperboloid shapes, and their focal length dictates the quality of the X-ray images that are produced, and examples of which are shown in Figs. 12 and 13. Chandra produces images with 0.3 arcsec resolution, XMM-Newton with 7 arcsecs, and SXT will produce images with 3–4 arcmin resolution (as was the case

Fig. 9 Assembly of XMM-Newton mirrors 58 nested shells

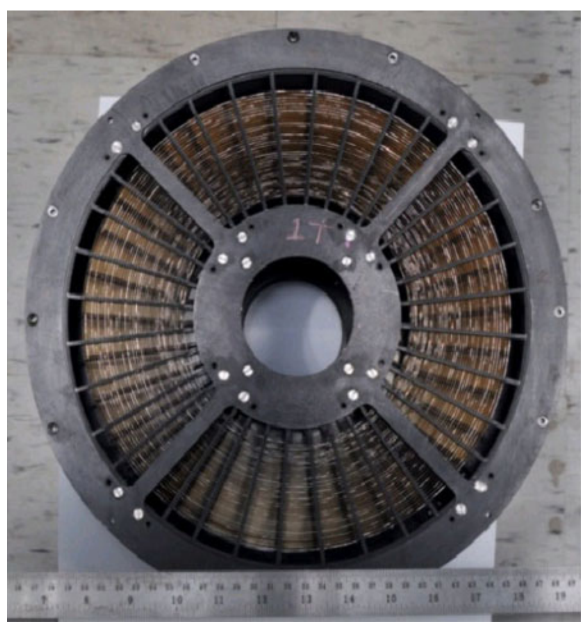

Fig. 10 Assembly of Astrosat SXT mirrors 40 nested shells (*top view*)

Fig. 11 Assembly of Astrosat SXT mirrors 40 nested shells (*side view*)

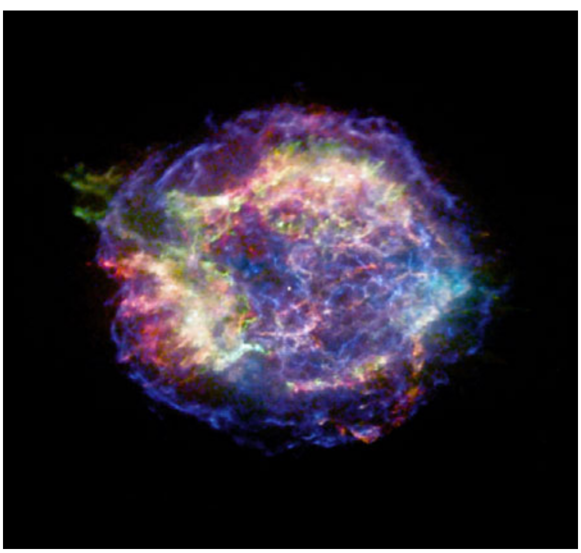

Fig. 12 X-ray image taken with CXO of a supenova remnant Casseopia A with *red color* showing low energy X-rays, *green color* for medium energy and *blue color* for high energy X-rays. Image is 8.91 arcmin across (about 26 light years) at a distance of 11,000 light years

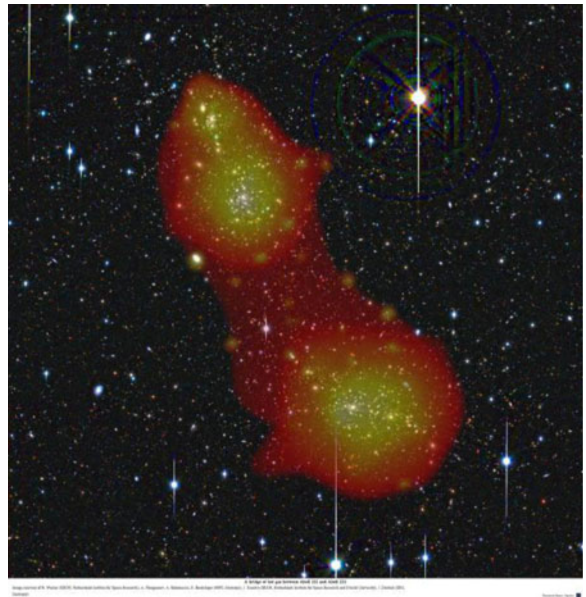

Fig. 13 X-ray image (overlaid on optical) taken with XMM-Newton of hot gas in a cluster of galaxies Abell 222 and Abell 223 and the X-ray bridge connecting the two clusters. The image size is 25 × 25 arcmin and the object is at a distance of 2,300 million light years

with ASCA). The fields of view are dictated by the number of detectors in the focal plane. The detectors generally used are specially cooled (-60 to -120°C) CCDs with large depletion depths and pixel size matching the spatial resolution of the telescope.

Hard X-ray mirrors: the new frontier

The telescopes described so far are useful only for soft X-rays ($E < 1\ 0$ keV). Presently hard X-ray astronomy uses either collimators or coded aperture masks to observe hard X-rays from astronomical sources. In these systems the internal detector background dominates the typical source fluxes because the collecting area and the detector areas are about the same. In a focusing system the collecting area can be 1,000 times the detector area improving the sensitivity enormously. Focusing of hard X-rays (with energies > 10 keV) using standard metal coatings is, however, difficult, since the grazing incidence angle decreases with energy, and for a reasonable focal length the system becomes impractically long and the field of view very small. The effective area of the mirror also decreases and nesting becomes difficult. However, fabrication of a large number of such small diameter telescopes using electroformed Ni shells is being pursued in USA for the next generation hard X-ray telescopes. Super-mirrors or mirrors that can reflect hard X-rays can also be made using multi-layered coatings. Bragg reflection from depth-graded multi-layers is used to increase the grazing angle over a broad energy range. Alternate layers of a high Z (W, Mb, Ni) and a low Z (C, Si) materials with high and low refractive indices, and with bi-layer thickness varying over a wide range have to be used for multi-layered coatings on the soft X-ray mirror. Typically the thinnest layers (which reflect the highest energy X-rays) are deposited first, so as to minimize absorption due to the overlying coatings. The multilayers are either replicated on to Al foils from glass surfaces in the same way as described above for a single layer, or coated directly on configured thin glass surfaces used as mirrors. Both the technologies are currently being pursued for the next generation hard X-ray telescopes. True imaging of X-rays in the energy range of 10–100 keV will further widen our horizons and help us explore the universe where non-thermal emission from cosmic X-ray sources dominates.

Acknowledgements I thank the NASA's Chandra X-ray Observatory Centre and the XMM-Newton Observatory Centre for making the images reproduced here available.

References

1. K.P. Singh, Techniques in X-ray astronomy I. Imaging telescopes. Resonance, June 2005, pp. 15–23
2. D. Attwood, *Soft X-rays and Extreme Ultraviolet Radiation: Principles and Applications* (Cambridge University Press, Edinburgh, UK, 2000), pp. 55–95
3. J.H. Underwood, D.T. Attwood, The renaissance of X-ray optics. Phys. Today, April 1984, pp. 44–50
4. B. Aschenbach, X-ray telescopes. Rep. Prog. Phys. **48**, 579 (1985)
5. P. Kirkpatrick, A.V. Baez, Formation of optical images by X-rays. J. Opt. Soc. Am. **38**, 766 (1948)
6. H. Wolter, Spiegelsysteme streifenden Einfalls als abbildene optiken fuer Roentgenstrahlen. Ann. Phys. **10**, 94 (1952)
7. H. Wolter, Verallgemeinerte schwarzschildsche spieglesysteme streifender reflexion als optiken fuer roentgenstrahlen. Ann. Phys. **10**, 286 (1952)
8. P.J. Serlemitsos, Conical foil X-ray mirrors—performance and projections. Appl. Opt. **20**, 1080 (1988)
9. N.J. Westergaard et al., Status of the development of a thin-foil high-throughput X-ray telescope for the Soviet spectrum X-gamma mission. Opt. Eng. **29**, 658 (1990)
10. S. Yang, J. Lalit, P.J. Serlemitsos, Conical thin foil X-ray mirror fabrication via surface replication. Proc. SPIE **2515**, 64 (1995)
11. P.J. Serlemitsos, S. Yang, Foil X-ray mirrors. Astrophys. Space Sci. **239**, 177 (1996)
12. H. Kunieda et al., X-ray telescope onboard Astro-E: optical design and fabrication of thin foil mirrors. Appl. Opt. **40**, 553 (2001)
13. K.-W. Chan, S. Yang, P.J. Serlemitsos, X-ray mirrors for the Astro-E2 mission. Proc. SPIE **4851**, 451 (2003)
14. L.G. Parratt, Surface studies of solids by total reflection of X-rays. Phys. Rev. **95**, 359 (1954)
15. A. Sagdeo, S.K. Rai, G.S. Lodha, K.P. Singh, N. Yadav, R. Dhawan, U. Tonpe, M.N. Vahia, X-ray characterization of thin foil gold mirrors of a soft X-ray telescope for ASTROSAT. Exp. Astron. **28**, 11 (2010)